A characteristic nonlinear distortion length for broadband Gaussian noise

Michael B. Muhlestein and Kent L. Gee

ARTICLES YOU MAY BE INTERESTED IN

A numerical investigation of passive acoustic mapping for monitoring bubble-mediated focused ultrasound treatment of the spinal cord
The Journal of the Acoustical Society of America **153**, 2271 (2023); https://doi.org/10.1121/10.0017836

Estimating cochlear impulse responses using frequency sweeps
The Journal of the Acoustical Society of America **153**, 2251 (2023); https://doi.org/10.1121/10.0017547

Fast grid-free strength mapping of multiple sound sources from microphone array data using a Transformer architecture
The Journal of the Acoustical Society of America **152**, 2543 (2022); https://doi.org/10.1121/10.0015005

Tensor dictionary learning for representing three-dimensional sound speed fields
The Journal of the Acoustical Society of America **152**, 2601 (2022); https://doi.org/10.1121/10.0015056

A steerable non-paraxial Gaussian beam expansion for a steerable parametric array loudspeaker
The Journal of the Acoustical Society of America **153**, 124 (2023); https://doi.org/10.1121/10.0016816

Testing the theoreticians
The Journal of the Acoustical Society of America **153**, R7 (2023); https://doi.org/10.1121/10.0017718

A characteristic nonlinear distortion length for broadband Gaussian noise

Michael B. Muhlestein[1,a] and Kent L. Gee[2]

[1]U.S. Army Engineer Research and Development Center, 72 Lyme Road, Hanover, New Hampshire 03777, USA

[2]Physics and Astronomy, Brigham Young University, N283 ESC, Provo, Utah 84602, USA

ABSTRACT:

The nonlinear evolution of high-amplitude broadband noise is important to the psychoacoustic perception, usually annoyance, of high-speed jet noise. One method to characterize the nonlinear evolution of such noise is to consider a characteristic nonlinear waveform distortion length for the signal. A common length scale for this analysis is the shock formation distance of an initially sinusoidal signal. However, application of this length scale to broadband noise, even with the amplitude and source frequency replaced with characteristic values, may lead to underestimates of the overall nonlinear waveform distortion of the noise as indicated by the skewness of the time derivative of the acoustic pressure (or derivative skewness). This paper provides an alternative length scale derived directly from the evolution of the derivative skewness of Gaussian noise that may be more appropriate when analyzing the nonlinear evolution of broadband noise signals. This Gaussian-based length scale is shown to be a useful metric for its relative consistency and its physical interpretation. Various analytical predictions of the evolution of the derivative skewness for an ensemble of numerical simulations of noise propagation are used to highlight various aspects of this new length scale definition. https://doi.org/10.1121/10.0017858

I. INTRODUCTION

An important application of nonlinear acoustic noise research is the radiation and propagation of high-amplitude broadband noise from high-speed jets. Research related to continuous random noise nonlinearities began in earnest in the 1970s (Ffowcs Williams, 1974; Pernet and Payne, 1971; Pestorius and Blackstock, 1974; Webster and Blackstock, 1978) and continued into the 1980s (Crighton and Bashforth, 1980; Gallagher and McLaughlin, 1981; McDaniel et al., 1980; Morfey and Howell, 1981; Sakagami et al., 1982; Watanabe and Urabe, 1981). Early studies particularly connected to nonlinear jet noise propagation include those by Blackstock, Ffowcs Williams et al., Gallagher and McLaughlin, Morfey and Howell, and Crighton and Bashforth. Recent years have seen renewed interest in understanding shock formation in noise radiated from supersonic jets (Baars et al., 2014; Fiévet et al., 2016; Petitjean et al., 2006; Pineau and Bogey, 2021) with direct application to both aircraft (Brouwer, 2008; Gee et al., 2016; McInerny et al., 2007; Murray and Lyons, 2016) and rockets (Gee et al., 2012; McInerny and Ölçmen, 2005). Some studies (Baars and Tinney, 2014; Gee et al., 2016; Murray and Lyons, 2016) have sought to connect shock physical properties to the psychoacoustic phenomenon, "crackle" (Ffowcs Williams et al., 1975).

Human perception of crackle in jet noise has been strongly correlated to the skewness of the time derivative of the acoustic pressure in a signal, or derivative skewness [see Gee et al. (2018) and references therein]. Skewness is a statistical metric characterizing the asymmetry of a distribution and may be written as

$$\mathrm{Sk}[X] = \frac{\langle X^3 \rangle}{\langle X^2 \rangle^{3/2}}, \tag{1}$$

where X is assumed to be a zero-mean variable (possibly random), and $\langle \cdot \rangle$ is the expected value of the argument. Furthermore, an increasing derivative skewness is closely associated with the wave distortion caused by the nonlinear propagation of high-amplitude waves (Muhlestein and Gee, 2011; Reichman et al., 2016a; Shepherd et al., 2011), thus, linking the importance of nonlinearity in such propagation to crackle.

The importance of nonlinearity in a propagating signal has traditionally been characterized by the ratio of two length scales, an absorption length and a nonlinear distortion length, often called the Gol'dberg number (Blackstock et al., 2008). An ideal nonlinear distortion length would be much larger than the absorption length, or the Gol'dberg number would be much less than one, if the effects of nonlinearity on acoustic propagation are negligible. It then follows from the above paragraph that there should be a connection between these length scales and the derivative skewness. However, the standard definitions of these two length scales were derived under the assumption of an initially sinusoidal signal (Blackstock et al., 2008), which means that any connection to the derivative skewness is only applicable to this non-stochastic signal. On the other hand, the simplicity of the sinusoidal signal allows some

a)Electronic mail: Michael.B.Muhlestein@erdc.dren.mil

exact solutions to be obtained, which in turn enable physical interpretations of the length scales.

A number of researchers have sought to extend the initially-sinusoidal-signal analysis to broadband noise signals by defining a characteristic frequency and amplitude for noise and substituting these values directly into the expressions for the length and absorption scales defined for sinusoidal signals (Baars *et al.*, 2016; Gurbatov and Rudenko, 2008; Muhlestein and Gee, 2011). The characteristic amplitude is usually taken to be the standard deviation of the pressure [also known as the root mean square (rms) amplitude for a zero-mean signal]. The characteristic frequency is more challenging to define and is usually taken to be either some "peak" or "central" frequency with little justification for the choice. However, these approaches are problematic due to the fact that the characters of sinusoidal and broadband noise distributions are fundamentally different. For example, the distributions for a sinusoid and a Gaussian process are plotted together in Fig. 1. Notice that the distribution for the sinusoid is bimodal with diverging peaks and finite in extent, while the distribution for the Gaussian process is unimodal and is infinite in extent. Since the skewness emphasizes the outliers of a distribution, it is reasonable to expect the evolution of the derivative skewness to be fundamentally different for initially sinusoidal signals and broadband noise signals.

In this paper, we take an alternative approach to defining the nonlinear distortion length (not the full Gol'dberg number, as an appropriate definition of the absorption length remains for future work). Rather than attempting to find a sinusoid that is somehow representative of broadband noise, we seek to derive a length scale directly from the statistics of the signals, especially the derivative skewness. This derivation is given in Sec. II. Section III then compares the standard and statistical length scales to an ensemble of numerical simulations. Finally, Sec. IV presents a concluding discussion.
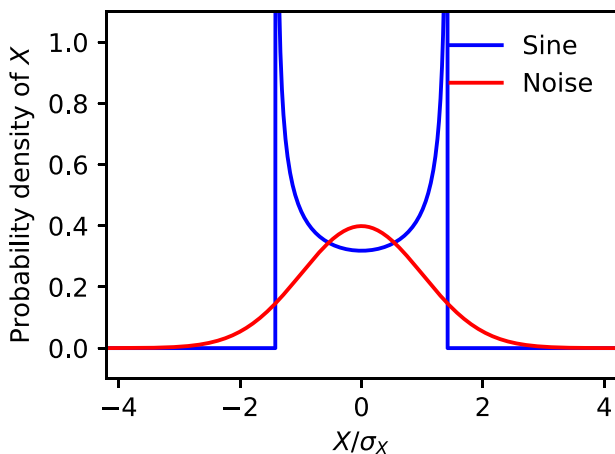

FIG. 1. (Color online) Probability density distributions for a sinusoid and a Gaussian process (X) normalized by the standard deviation (σ_X).

II. THEORETICAL DEVELOPMENT

The statistical skewness of the time derivative of the acoustic pressure (hereafter just called pressure), or the derivative skewness, may be obtained as a weighted integration of the pressure time-derivative probability density function measured at a distance x from the source, or "temporal slope density," and notated as $\rho_x(\dot{p})$, where p is the pressure and the over-dot denotes the time derivative. Muhlestein and Gee (2016) found that the evolution of the temporal slope density may be found exactly for arbitrary signals in the case of lossless and planar sound propagation before shock formation using the Earnshaw solution to the Burgers equation. Since their results are critical to the development below, a brief summary of their results that are pertinent to this work is provided. This summary is followed by a careful analysis of the special case of initially Gaussian-distributed noise before finally deriving the characteristic nonlinear distortion length.

A. Summary of results from Muhlestein and Gee (2016)

One way to interpret the Earnshaw solution to the inviscid Burgers equation (Blackstock *et al.*, 2008) is that the retarded time of arrival of the individual amplitude points varies as a function of the source amplitude and measurement position but that the measured amplitude remains the same as the source pressure. Thus, each point of the propagated pressure waveform (retarded time of arrival and pressure amplitude) depends only on a single point of the source waveform. An important point is that the new retarded time of arrival is simply the source time of arrival plus a correction factor that does not depend on the source time of arrival. Therefore, the change in the time of arrival of every point with the same source pressure amplitude will also be the same. Using these facts, Muhlestein and Gee were able to calculate the evolution of the pressure time derivatives and their infinitesimal durations as a function of propagation distance and then obtain the propagated temporal slope density as a function of the source temporal slope density and the propagation distance. The resulting expression, adapted from Eq. (7) from Muhlestein and Gee (2016), may be written as

$$\rho_x(\dot{p}) = \rho_0\left(\frac{\dot{p}}{1 + (\beta/\rho_0 c_0^3)x\dot{p}}\right)\frac{1}{\left[1 + (\beta/\rho_0 c_0^3)x\dot{p}\right]^3}, \quad (2)$$

where β is the coefficient of nonlinearity, ρ_0 (without arguments) is the equilibrium mass density, and c_0 is the small-signal sound speed. The ratio $\beta/\rho_0 c_0^3$ is so common throughout this work, it will be given its own symbol, η, such that we may write

$$\rho_x(\dot{p}) = \rho_0\left(\frac{\dot{p}}{1 + \eta x\dot{p}}\right)\frac{1}{\left[1 + \eta x\dot{p}\right]^3}. \quad (3)$$

Note that η has units of $[\text{m (Pa/s)}]^{-1}$.

The skewness of a variable X may be expressed as

$$\text{Sk}[X] = \frac{\mu^{(3)}}{\left[\mu^{(2)}\right]^{3/2}}, \qquad (4)$$

where $\mu^{(n)}$ is the nth central moment of the distribution of X. Assuming X is a zero-mean process (usual for acoustical phenomena), we may write

$$\mu^{(n)} = \int_{-\infty}^{\infty} \zeta^n \rho(\zeta)\, d\zeta, \qquad (5)$$

where $\rho(\zeta)$ is the probability density function for X. Thus, in principle, the derivative skewness may be calculated by using $\dot{p}$ for X and using $\rho_x(\dot{p})$ from Eq. (3). The central moments for $\rho_x(\dot{p})$ may not be explicitly evaluated in general. However, if $\rho_x(\dot{p})$ is expanded in a power series about $x = 0$, the central moments may be written as a linear combination of the central moments at the source as [Muhlestein and Gee (2016), Eq. (10)]

$$\mu_x^{(n)} = \sum_{k=0}^{\infty} \frac{(n-2+k)!}{(n-2)!k!} (\eta x)^k \mu_0^{(n+k)}, \qquad (6)$$

where $\mu_x^{(n)}$ is the nth central moment of the pressure time derivative measured at position x. Thus, the derivative skewness may be written as the ratio of two infinite power series in terms of x, which may in turn be expressed as a single power series in terms of x. The first two terms may be written explicitly as [Muhlestein and Gee (2016), Eq. (11)]

$$\text{Sk}[\dot{p}] = \frac{\mu_0^{(3)}}{\left[\mu_0^{(2)}\right]^{3/2}} + \frac{4\mu_0^{(2)}\mu_0^{(4)} - 3\left[\mu_0^{(3)}\right]^2}{2\left[\mu_0^{(2)}\right]^{5/2}} \eta x + O(x^2). \qquad (7)$$

B. Definition of a statistical nonlinear distortion length for initially Gaussian noise

A characteristic distortion length should represent the rate of change of the quantity in question as a function of position. We therefore define the statistical nonlinear distortion length for an arbitrary signal to be the inverse of the gradient of the derivative skewness as measured at the source. Written mathematically, the statistical nonlinear distortion length D of a pressure waveform p may be expressed as

$$D = \left[\left.\frac{\partial\text{Sk}[\dot{p}]}{\partial x}\right|_{x=0}\right]^{-1} = \frac{2\left[\mu_0^{(2)}\right]^{5/2}}{4\mu_0^{(2)}\mu_0^{(4)} - 3\left[\mu_0^{(3)}\right]^2} \eta^{-1}, \qquad (8)$$

where the second equality makes use of Eq. (7).

Using the results presented above, the derivative skewness for an initially sinusoidal signal may be written as

$$\text{Sk}[\dot{p}_S] = \frac{3}{\sqrt{2}} \eta\omega p_0 x + \frac{13}{8\sqrt{2}} (\eta\omega p_0 x)^3 \\ + \frac{165}{128\sqrt{2}} (\eta\omega p_0 x)^5 + O(x^7), \qquad (9)$$

where the subscript S denotes a sinusoidal process, ω is the angular frequency of the source sinusoid, and p_0 is the source pressure amplitude. This expression is the same as that found in Eq. (18) of Muhlestein and Gee (2016), except that their expression included a minor numerical error: The cubic coefficient was given as $13/32\sqrt{2}$, which is a factor of 4 too small. Written in terms of the shock formation distance (SFD), or the distance a wave needs to propagate without losses before an acoustic shock is formed, for an initially sinusoidal signal,

$$\bar{x}_S = \frac{1}{\eta\omega p_0}, \qquad (10)$$

Eq. (9) becomes

$$\text{Sk}[\dot{p}_S] = \frac{3}{\sqrt{2}}\frac{x}{\bar{x}_S} + \frac{13}{8\sqrt{2}}\left(\frac{x}{\bar{x}_S}\right)^3 + \frac{165}{128\sqrt{2}}\left(\frac{x}{\bar{x}_S}\right)^5 \\ + O\left(\left[\frac{x}{\bar{x}_S}\right]^7\right). \qquad (11)$$

Muhlestein (2013) derived an exact expression for the derivative skewness of an initially sinusoidal signal, given by

$$\text{Sk}[\dot{p}_S] = \frac{2(1-\sigma^2)^{3/2} + 3\sigma^2 - 2}{(1-\sigma^2)^{3/4}\left(1 - \sqrt{1-\sigma^2}\right)^{3/2}}, \qquad (12)$$

where $\sigma = x/\bar{x}_S$. Expanding Eq. (12) about $\sigma = 0$ recovers Eq. (11), so the derivative skewness may be expanded in a power series of the normalized propagation distance.

Muhlestein and Gee (2016) also calculated the derivative skewness for a noise signal with Gaussian statistics for the initial pressure time derivative, given by

$$\text{Sk}[\dot{p}_G] = 6\eta\,\text{std}[\dot{p}]x + 33(\eta\,\text{std}[\dot{p}]x)^3 \\ + \frac{1305}{4}(\eta\,\text{std}[\dot{p}]x)^5 + O(x^7), \qquad (13)$$

where the subscript G denotes a Gaussian process, and $\text{std}[\cdot]$ is the standard deviation of its argument. [Note there is another minor numerical error in the expression given by Muhlestein and Gee (2016) in Eq. (22), where the coefficient of the x^5 term is $2115/4$ rather than $1305/4$ given here.] In general, the nth term of Eq. (13) may be written as

$$\frac{c_n}{4^{n-2}}(\eta\,\text{std}[\dot{p}]x)^{2n-1}, \qquad (14)$$

where the first six values of c_n are, sequentially, $3/2$, 33, 1305, $65\,610$, $3\,872\,745$, and $259\,326\,846$.

Since much of the physical intuition surrounding nonlinear distortion has been built around the case of an initially sinusoidal signal, it becomes desirable to connect the analysis of a noise signal to that case. We therefore define a characteristic nonlinear distortion length $\bar{x}_G$ such that the normalized slope of the derivative skewness predictions match at $x \to 0$, or

Michael B. Muhlestein and Kent L. Gee

$$\frac{3}{\sqrt{2}}\frac{1}{\bar{x}_G} = 6\eta\, \text{std}[\dot{p}], \qquad (15)$$

which then implies

$$\bar{x}_G = \frac{1}{2\sqrt{2}\eta\, \text{std}[\dot{p}]}. \qquad (16)$$

It is worth noting that in the limit that the source signal becomes sinusoidal, we find that $\bar{x}_G \to \bar{x}_S/2$ because $\text{std}[\dot{p}_S] = \omega p_0/\sqrt{2}$. The fact that $\bar{x}_G$ does not reduce to $\bar{x}_S$ suggests that using other results derived from initially sinusoidal signals to interpret noise signals may be similarly inaccurate.

This point may be further explored by substituting $\bar{x}_G$ into Eq. (13) above. The derivative skewness for Gaussian noise may be written as

$$\text{Sk}[\dot{p}_G] \approx \frac{3}{\sqrt{2}}\frac{x}{\bar{x}_G} + \frac{33}{16\sqrt{2}}\left(\frac{x}{\bar{x}_G}\right)^3 + \frac{1305}{512\sqrt{2}}\left(\frac{x}{\bar{x}_G}\right)^5. \qquad (17)$$

Notice that the term in Eq. (17) that is cubic in x does not have the same form as the cubic term as the derivative skewness for the sinusoidal source in Eq. (11). In fact, the coefficient for the cubic term for a noise source is about 1.27 times the coefficient for a sinusoidal source. Similar differences occur for higher order terms; see Fig. 2, which shows the derivative skewness to 11th order in x as a function of the scaled distance (by $\bar{x}_S$ for initially sinusoidal signals and by $\bar{x}_G$ for noise signals). (The 11th-order approximation is the most useful approximation for finite signals that do not have amplitudes above 3.8 standard deviations; see Appendix for details.) These differences provide quantifiable evidence that the evolution of the statistics for initially Gaussian noise is fundamentally distinct from the evolution of the statistics for an initially sinusoidal signal. This result
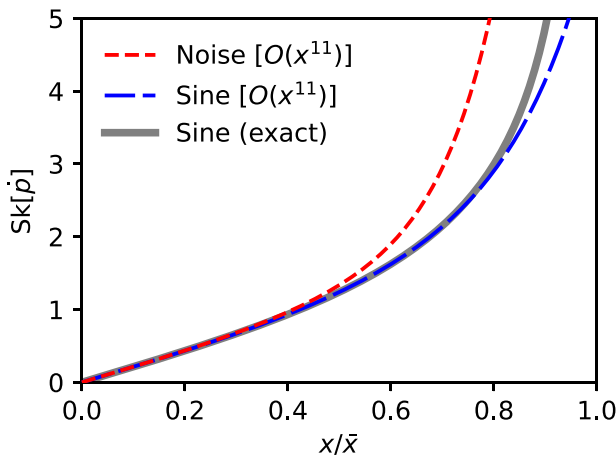

FIG. 2. (Color online) Approximate derivative skewness for initially Gaussian and sinusoidal signals as a function of scaled distance using an 11th-order asymptotic series. The exact derivative skewness for an initially sinusoidal signal [as given in Eq. (12)] is included as well for reference. The scaling factor for the distance is $\bar{x}_S$ for the initially sinusoidal signal and is $\bar{x}_G$ for the initially Gaussian signal.

is similar to that found by Rudenko [as reported by Gurbatov and Rudenko (2008)], where the evolution of the second and third harmonics of narrowband noise was found to be distinct from the same for pure tones. One must therefore use caution when using intuition developed from analyzing initially sinusoidal signals to interpret the statistics of nonlinearly propagating broadband noise signals.

It is important to recall that other definitions for a characteristic nonlinear distortion length for noise have already been posited, and $\bar{x}_G$ should be compared with these earlier definitions. Perhaps the most obvious choice is the true SFD, which may be written exactly for lossless planar propagation as

$$\text{SFD} = \frac{\rho_0 c_0^3}{\beta \dot{p}_{\text{max}}}, \qquad (18)$$

where $\dot{p}_{\text{max}}$ is the peak pressure time derivative. Another definition was given by Gurbatov and Rudenko (2008) using the SFD for a sine wave, $\bar{x}_S$, as a guide,

$$\bar{x}_C = \frac{\rho_0 c_0^3}{\beta \omega_c \text{std}[p]}, \qquad (19)$$

where ω_c is a characteristic or central frequency. [Muhlestein and Gee (2011) notated this definition as $\bar{x}_G$; please note that $\bar{x}_G$ in this paper will be used exclusively to refer to the definition given in Eq. (16).] The SFD relies on the extremum of a particular distribution and, therefore, is not likely to be either consistent for different stochastic signals or representative of the overall signal. The characteristic definition $\bar{x}_C$ does not provide a specific definition for what is meant by a ω_c, so *ad hoc* definitions are usually provided and may lead to widely disparate values for a given signal. Furthermore, $\bar{x}_C$ notably does not rely on the statistics of the pressure time derivative, but instead on the statistics of the pressure magnitude. Since the statistics of the pressure magnitude do not vary with lossless planar propagation before shock formation (Rudenko and Chirkin, 1975; Webster and Blackstock, 1979), $\bar{x}_C$ may not be sensitive to pre-existing distortion in the source signal.

As a final comment in this section, the results derived here for planar propagation may be easily extended to the case of diverging waves using existing expressions (Blackstock *et al.*, 2008). The SFD for spherical and cylindrical sinusoidal waves may be written, respectively, as

$$\text{SFD}_{\text{sph}} = r_0 \exp\left(\frac{\rho_0 c_0^3}{\beta \omega p_0 r_0}\right), \qquad (20)$$

$$\text{SFD}_{\text{cyl}} = r_0 \left(1 + \frac{\rho_0 c_0^3}{2\beta \omega p_0 r_0}\right)^2, \qquad (21)$$

where r_0 is the reference radius. These expressions are obtained by taking the generalized Burgers equation for a lossless fluid with one-dimensional spreading, making a

change of variables in the pressure and position, obtaining the usual planar Burgers equation for planar propagation, determining the SFD, and inverting to the original coordinates. None of these steps involve modifications of the time derivative, and the statistics of the reference signal (magnitude and time derivative) remain unchanged. Thus, the SFD expressions may be readily changed to $\bar{x}_G$ expressions by simply replacing ωp_0 with $2\sqrt{2}\text{std}[\dot{p}]$ (where $\text{std}[\dot{p}]$ is evaluated at $r = r_0$),

$$\bar{x}_{G,\text{sph}} = r_0 \exp\left(\frac{\rho_0 c_0^3}{2\sqrt{2}\beta\text{std}[\dot{p}]r_0}\right), \quad (22)$$

$$\bar{x}_{G,\text{cyl}} = r_0\left(1 + \frac{\rho_0 c_0^3}{4\sqrt{2}\beta\text{std}[\dot{p}]r_0}\right)^2. \quad (23)$$

Similar substitutions can be made for expressions of the SFD for generally diverging waves in lossless media (Hamilton, 2016).

III. FINITE-LENGTH SIGNALS: JET-LIKE NOISE

Section II focused on results assuming idealized statistical distributions and an infinitesimal sampling rate. It may be helpful to analyze a more realistic example: a finite-length numerically generated jet-like Gaussian noise signal with a finite sampling rate. Military aircraft can create jets with radiated noise that has a central frequency close to 150 Hz, a relatively broad spectrum, and overall sound pressure levels on the order of 155 dB (Leete *et al.*, 2021; Wall *et al.*, 2012). Using these metrics as a guide, 2.73 s of a Gaussian-distributed noise sample was generated with a sampling rate of 96 000 samples/s, using a fifth-order Butterworth bandpass filter from 75 to 300 Hz, and the resulting signal was normalized to have an overall sound pressure level of 155 dB. Using $\omega_c = 2\pi150 \text{ s}^{-1}$ for the characteristic angular frequency, the signal then has $\bar{x}_C = 38.1$ m by definition.

A portion of the waveform of the jet-like Gaussian source noise is shown in Fig. 3 as a function of retarded time at the source, the SFD, $\bar{x}_G$, and $\bar{x}_C$. The source noise signal was propagated using the Earnshaw solution (distortion of the time series leaving the pressure amplitudes the same) and the equal-area rule to account for weak shocks (Blackstock *et al.*, 2008). Qualitatively, the waveform at the SFD (7.3 m for this instance) has steepened significantly, but no shocks are apparent in the portion that is shown (chosen to be representative of the bulk of the signal). The lack of shocks is expected, as the SFD occurs when the very first shock forms, and it is unlikely that a random sample would include that shock. The waveform at the SFD and at $\bar{x}_G$ (10.0 m for this instance) are quite similar, but at this point, more shocks have formed (3.7 shocks/s), although they still do not appear in the small portion shown. On the other hand, the waveform at $\bar{x}_C$ (38.1 m, the same for all instances) contains many shocks in the portion shown, and the average number of shocks/s is 187.5. Note that the "characteristic"
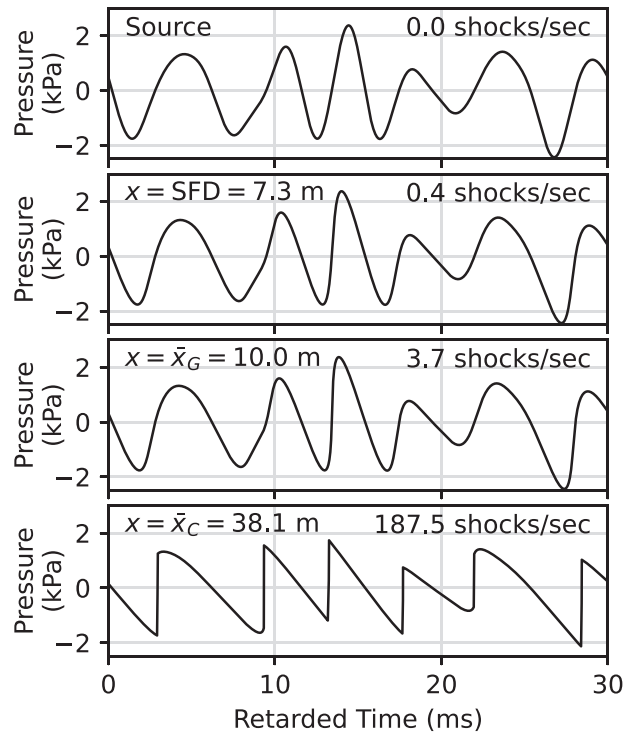

FIG. 3. A portion of one instance of the randomly generated jet-like noise at (sequentially from top to bottom) the source, SFD (7.3 m), $\bar{x}_G$ (10.0 m), and $\bar{x}_C$ (30.5 m) as a function of the retarded time. The number of shocks/s in the whole waveform at each location is also given in the respective plot.

frequency of the signal is assumed to be 150 Hz, so the rate of shocks is greater than the assumed signal frequency.

The temporal slope density of the noise sample described above is shown in Fig. 4. On average, the source temporal slope density resembles a Gaussian distribution to about 3.8 standard deviations, so comparisons with analytical theory will be limited to the 11th-order asymptotic approximation, as discussed in the Appendix. Similar to the waveforms, the distributions at the SFD and at $\bar{x}_G$ are rather similar to each other, with diminished numbers of very large-magnitude negative slopes, an increase in low-magnitude negative slopes, and a significant increase in high-magnitude positive slopes (associated with shock formation) compared to the Gaussian source distribution. The
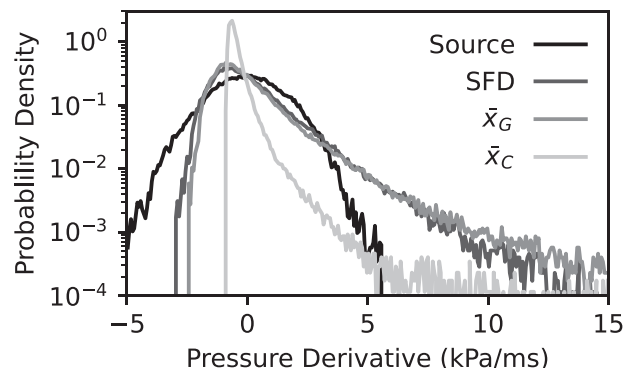

FIG. 4. Slope density of an instance of the randomly generated jet-like noise at the source, the SFD, $\bar{x}_G$, and $\bar{x}_C$, as defined in the main text.

distribution at $\bar{x}_C$ exhibits the same overall trends, but to a much larger degree than for the other two distorted signals. In addition, the presence of excess attenuation at shock fronts due to weak-shock theory has led to a change of the overall content in general, such that the high-magnitude positive slopes are not as numerous as in the other cases. Thus, the statistical character of the noise at $\bar{x}_C$ is markedly different from the statistical character at the SFD and $\bar{x}_G$.

A greater understanding of the use of finite signals with finite sampling rates may be obtained by analyzing the statistics of an ensemble of samples. Thus, 1000 random samples were generated using the same method as described above. Due to their random nature, each of the noise samples has a unique SFD. The minimum, 25th percentile, median, 75th percentile, and maximum value of the SFD are, respectively, 5.45, 7.06, 7.50, 7.92, and 9.40 m. The distribution of the values of $\bar{x}_G$ is comparatively much tighter, with the minimum, 25th percentile, median, 75th percentile, and maximum values being given by, respectively, 9.53, 9.80, 9.87, 9.95, and 10.18 m. These values are summarized visually in Fig. 5. Note that the $\bar{x}_G$ values are all larger than the SFD values; this feature highlights the fact that $\bar{x}_G$ characterizes the importance of nonlinearity on the overall waveform rather than just on the most extreme points, as the SFD does. For comparison, recall that $\bar{x}_C$ is equal to 38.1 m for every case, which is much larger than any of the values of the SFD or $\bar{x}_G$.

This ensemble of jet-like noise samples may also be used to show the connection between the different nonlinear distortion lengths and the derivative skewness. Each of the 1000 samples was numerically propagated to 11 m, or just beyond the largest value of $\bar{x}_G$, and the derivative skewness was calculated as a function of position. For comparison, an initially sinusoidal source waveform was also generated and propagated. The sinusoidal source has a frequency of 150 Hz and an amplitude such that the gradient of its derivative skewness at the source is equal to the gradient of the median derivative skewness of the noise signals, or 4.34 kPa, and an overall sound pressure level of 163.7 dB. This choice of the amplitude and frequency for the sinusoidal source then leads to $\bar{x}_S$ being equal to the median of $\bar{x}_G$.

The full range (gray patch, labeled "Num. Noise Range"), the inter-quartile range (yellow patch, labeled "Num. Noise IQR"), and median (thick black line, labeled "Num. Noise Med.") of the derivative skewness of the

numerically propagated noise as a function of the propagation distance are plotted in Fig. 6, as well as the derivative skewness of the numerically propagated initial sinusoid (thick dashed line). The noise signals did not have perfectly zero derivative skewness at the source (although the ensemble median converges on zero), but the rate of increase for the derivative skewness as a function of position was nearly identical for all cases. Thus, a tight distribution of derivative skewness values appears close to the source. As each sample approaches its own SFD, the derivative skewness value starts to diverge, but since each sample has a unique SFD, the distribution of derivative skewness values broadens rapidly with increasing propagation distance. For distances beyond the analytical SFD, the derivative skewness goes, in principle, to infinity, although in practice, the finite sampling rate leads to a finite maximum derivative skewness (Reichman *et al.*, 2016b). To avoid numerical errors and singularities, the plot of the derivative skewness is limited to skewness values between 0 and 10. Thus, the statistical measures shown in Fig. 6 are only strictly valid prior to the first SFD, which is noted in the figure. The median and maximum SFD values are also shown for reference.

The 11th-order predictions for the derivative skewness for initially Gaussian noise [see Eq. (17)] and for initially sinusoidal signals [see Eq. (11)] are also plotted in Fig. 6. For these plots, the median value of $\bar{x}_G$ was used as the characteristic nonlinear distortion length for both initially Gaussian noise and sinusoidal signals, such that the gradients of the derivative skewness predictions close to the source would be identical. Both of the analytical expansions agree with the median noise derivative skewness near the source, but the sinusoidal prediction eventually diverges, followed later by the noise prediction. The prediction assuming an initially sinusoidal signal first has relative error compared to the median greater than 1% at 2.6 m from the source. The prediction assuming an initial Gaussian distribution varies slightly around the median and first has a relative error greater than 1% at 4.9 m. On the other hand, the first
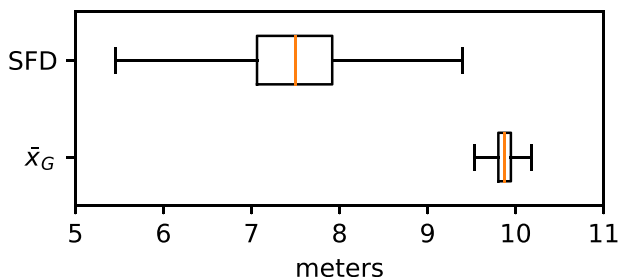
FIG. 5. (Color online) Box and whisker plots for the distributions of the individual SFD and $\bar{x}_G$ for the source Gaussian noise signals.
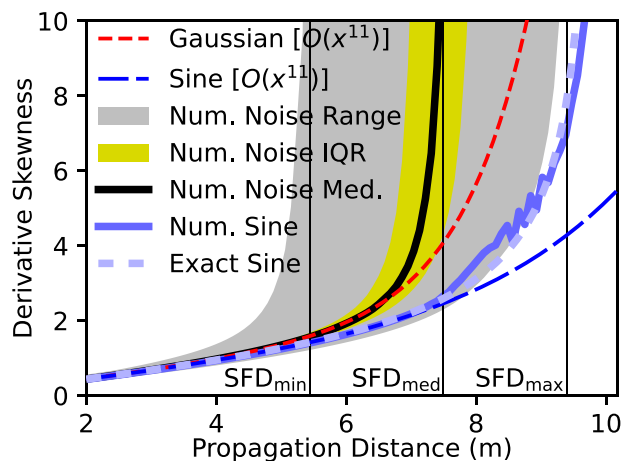
FIG. 6. (Color online) Derivative skewness of the numerically generated signals as a function of propagation distance. See the main text for a full explanation of the figure.

J. Acoust. Soc. Am. **153** (4), April 2023

Michael B. Muhlestein and Kent L. Gee   2267

point at which the sinusoidal expansion has a relative error greater than 1% compared to the initially sinusoidal numerical prediction (and the exact solution, also shown) occurs at 8.3 m, while assuming an initially Gaussian distribution first has a relative error greater than 1% at 1.6 m. It is interesting that the analytical predictions for the initially Gaussian noise and the initially sinusoidal signal both begin to diverge from their respective numerical examples at roughly the same derivative skewness value, around 2. Thus, the divergence of the analytical from the numerical values may be associated with the fact that the analytical values are limited to 11th-order rather than some inaccuracy of the analytical method.

This numerical example helps elucidate a number of relevant points. First, the SFD is a poor nonlinear distortion length, as it has a relatively broad distribution of values and does not correlate well with the overall distortion of a propagating noise waveform. On the other hand, $\bar{x}_G$ has a relatively tight distribution, even when defining a noise waveform using pressure statistics such as overall sound pressure level and spectrum rather than using pressure time-derivative statistics. The overall magnitude of $\bar{x}_G$ is larger than the SFD magnitudes, which correlates better with overall nonlinear distortion of a noise waveform. Another important point is that the classic distortion length for noise defined by Gurbatov and Rudenko (2008), $\bar{x}_C$, is consistently much larger than either the SFD or $\bar{x}_G$ and seems to be correlated more with a regime with well-established shocks and is, therefore, not appropriate to represent the initial distortion of a noise waveform.

IV. CONCLUDING DISCUSSION

This paper has shown that the nonlinear evolution of initially sinusoidal signals is similar but fundamentally distinct from the nonlinear evolution of initially Gaussian-distributed noise signals. This distinction was demonstrated by comparing the evolution of the skewness of the time derivative of the acoustic pressure, or derivative skewness, using both analytical and numerical means. To properly account for the source waveform statistics, a new nonlinear length scale, $\bar{x}_G$, defined in Eq. (16), was derived. The choice of $\bar{x}_G$ enables a consistent length scale that characterizes the overall nonlinear waveform distortion of broadband noise signals.

While this paper has focused on lossless propagation, it is likely that the broadband nature of noise will lead to additional complications with the definition of a characteristic absorption length and, in turn, a characteristic Gol'dberg number. The results in this paper alone would suggest a decreased Gol'dberg number, but the nonlinear frequency dependence of linear absorptive processes introduces complications that require additional study. It may be important to develop a Gol'dberg number-like spectrum to accurately describe the importance of nonlinearity for broadband signals. This development could be then used to build upon the work of, e.g., Baars *et al*. (2016) to provide greater

understanding of the relative importance of nonlinearity to linear absorption in jet noise.

APPENDIX: MATHEMATICAL AND PRACTICAL NOTES ON USING THE GAUSSIAN DISTRIBUTION

It is important to caveat the above analysis with the note that there is no guarantee that either of the two series in the derivative-skewness ratio of Eq. (6) converge. Indeed, for an initially Gaussian distribution,

$$\rho_{G0}(\dot{p}) = \frac{1}{\text{std}_0(\dot{p})^2\sqrt{2\pi}}\exp\left(-\frac{\dot{p}^2}{2\text{std}_0(\dot{p})^2}\right), \qquad (A1)$$

neither of the two series converge. To show this, consider the moment integrals for $x \neq 0$ written as

$$\mu_x^{(n)} = \int_{-1/\eta x}^{\infty} \frac{\zeta^n \, d\zeta}{[1+\eta x\zeta]^3} \frac{1}{\text{std}_0(\dot{p})\sqrt{2\pi}}\exp\left[\frac{-\zeta^2/[1+\eta x\zeta]^2}{2\text{std}_0(\dot{p})^2}\right], \qquad (A2)$$

where the lower bound to the integral is explained by Muhlestein and Gee (2016) and is immaterial to the present discussion. As $\zeta \to \infty$, the integrand approaches

$$\frac{\zeta^{n-3}/(\eta x)^2}{\eta x \, \text{std}_0(\dot{p})\sqrt{2\pi}}\exp\left[-\frac{1}{2[\eta x \, \text{std}_0(\dot{p})]^2}\right]. \qquad (A3)$$

For $n = 2$ the integrand tends toward a ζ^{-1} dependence, which diverges. For any integer $n > 2$, the integrand approaches either a non-zero constant or grows and is always positive, leading to divergent integrals. Thus, both $\mu_x^{(2)}$ and $\mu_x^{(3)}$ for the initially Gaussian distribution diverge for any $x > 0$.

Another way to think about the divergence of the initially Gaussian-distributed noise moments is that a Gaussian distribution has support over all the real numbers. Thus, an infinitely long signal would exhibit arbitrarily large pressure time derivatives, and a shock must already appear somewhere in the signal at the start. For any $x > 0$, the requirement that the signal does not pass the shock formation distance is, therefore, not fulfilled. However, physical noise signals are not truly Gaussian and have support over a finite domain of the real numbers. On the other hand, the Gaussian distribution is a good approximation for the temporal slope density function of real signals for slopes close to zero. The lowest statistical moments of both the Gaussian distribution and a physical unimodal signal, such as jet noise, will be dominated by the influence of the main peak of the distribution, while the higher moments will be dominated by the tails. Therefore, for sufficiently low-order

Michael B. Muhlestein and Kent L. Gee

moments, the Gaussian distribution is a good substitute for a physical unimodal signal. Furthermore, one may conclude from Eq. (10) of Muhlestein and Gee (2016) that the largest moment in the coefficient of σ^n (and so x^n) in the derivative skewness of an arbitrary distribution (so n is not limited to being odd) is the moment of order $n + 3$.

Taken together, these facts suggest that there is some odd integer k such that neglecting the terms $O(x^k)$ in Eq. (13) and keeping all other terms will provide the best estimate of the derivative skewness of real noise using a Gaussian distribution. The closer the slope density function of the noise resembles a Gaussian distribution, the better the approximation will be. The exact value of k depends on the noise signal in question, but a full analysis is tangential to the purpose of this paper; consequently, one will not be explored here. However, one may estimate a value of k by looking at the error of using the full Gaussian distribution compared to a truncated one (see Fig. 7) when calculating statistical moments. The truncated Gaussian distribution used here is defined as

$$\rho_{GT}(X, X_{max}) = \begin{cases} Ne^{-X^2/2}, & |X| \leq X_{max}, \\ 0, & |X| > X_{max}, \end{cases} \quad (A4)$$

where N is the normalization constant necessary to make the integral of the distribution equal to one, X is the random variable divided by the Gaussian standard deviation, and X_{max} is the truncation standard deviation. In the limit $X_{max} \to \infty$, the normalization constant is $N \to 1/\sqrt{2\pi}$, and the truncated Gaussian distribution approaches the full Gaussian distribution. The normalized error of using the full Gaussian distribution to estimate the nth moment instead of the truncated Gaussian distribution with a truncation standard deviation of X_{max} may then be written as

$$E_n = 1 - \frac{\mu_G^{(n)}}{\mu_{GT}^{(n)}} = 1 - \frac{1}{N\sqrt{2\pi}} \frac{\int_{-\infty}^{\infty} X^n e^{-X^2/2}}{\int_{-X_{max}}^{X_{max}} X^n e^{-X^2/2}}. \quad (A5)$$
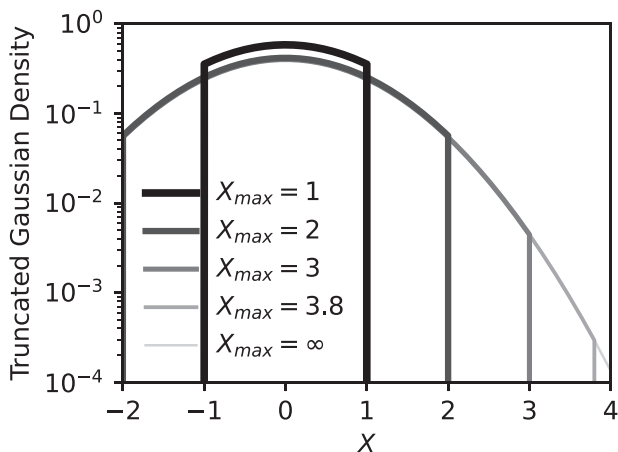

FIG. 7. Probability density functions for truncated Gaussian distributions. The truncation standard deviation is denoted by X_{max}.
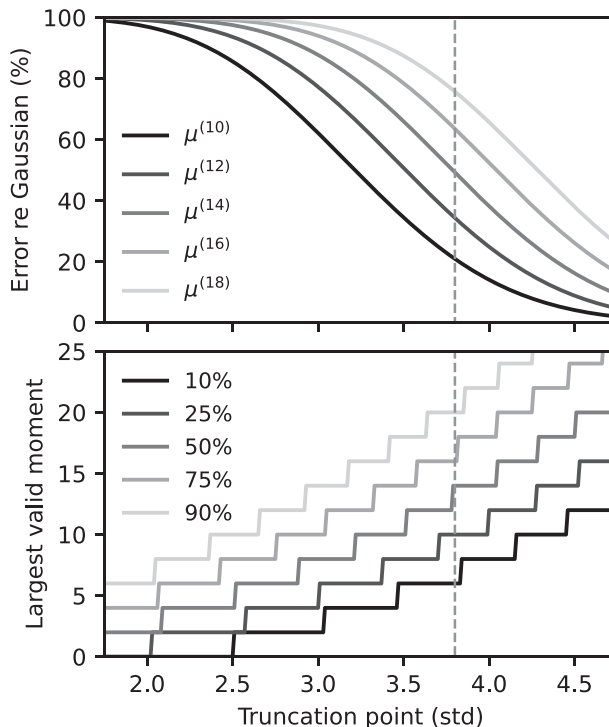

FIG. 8. (Top) Error for using a full Gaussian distribution for estimating the nth moment relative to using a truncated Gaussian distribution as a function of the truncation standard deviation for several values of n. (Bottom) Largest moment for which the error of using the full Gaussian distribution instead of the truncated distribution is less than a particular value for several of these limiting error values.

The normalized error E_n is shown in the top plot of Fig. 8 as a function of X_{max} for several values of n. As the value of n increases, the error increases at a fixed value of X_{max}. For all values of n, the error approaches 100% at $X_{max} \to 0$ and approaches 0% as $X_{max} \to \infty$ and varies smoothly and monotonically between these two limits. Thus, for any finite error limit, there is some integer m such that the error associated with the moment $\mu^{(n)}$ is above this error limit for all $n > m$. The bottom plot of Fig. 8 shows the smallest value of m as a function of X_{max} for several error limits. For the special case of $X_{max} = 3.8$, which is relevant below, we find that $m = 14$. Since the skewness relies on the third central moment, the ability to approximate moments up to the 14th source moment allows us to use the full Gaussian to describe the derivative skewness up to 11th order in x [i.e., using Eq. (13)].

Baars, W. J., and Tinney, C. E. (**2014**). "Shock-structures in the acoustic field of a Mach 3 jet with crackle," J. Sound Vib. **333**(12), 2539–2553.

Baars, W. J., Tinney, C. E., and Hamilton, M. F. (**2016**). "Piecewise-spreading regime model for calculating effective Gol'dberg numbers for supersonic jet noise," AIAA J. **54**(9), 2833–2842.

Baars, W. J., Tinney, C. E., Wochner, M. S., and Hamilton, M. F. (**2014**). "On cumulative nonlinear acoustic waveform distortions from high-speed jets," J. Fluid Mech. **749**, 331–366.

Blackstock, D. T., Hamilton, M. F., and Pierce, A. D. (**2008**). "Progressive waves in lossless and lossy fluids," in *Nonlinear Acoustics*, edited by M. F. Hamilton and D. T. Blackstock (Acoustical Society of America, New York), pp. 65–150.

Brouwer, H. H. (**2008**). "On the effect of nonlinear propagation on perceived jet noise levels," Aerosp. Sci. Technol. **12**(1), 74–79.

Crighton, D., and Bashforth, S. (**1980**). "Nonlinear propagation of broadband jet noise," in *Proceedings of the 6th Aeroacoustics Conference*, June 4–6, Hartford, CT.

Ffowcs Williams, J. E. (**1974**). "Nonlinear generation of secondary waves in fluids," in *Finite-Amplitude Wave Effects in Fluids: Proceedings of the 1973 Symposium, Copenhagen* (IPC Science and Technology, Guildford, UK), pp. 9–18.

Ffowcs Williams, J. E., Simson, J., and Virchis, V. J. (**1975**). " 'Crackle': An annoying component of jet noise," J. Fluid Mech. **71**(2), 251–271.

Fiévet, R., Tinney, C. E., Baars, W. J., and Hamilton, M. F. (**2016**). "Coalescence in the sound field of a laboratory-scale supersonic jet," AIAA J. **54**(1), 254–265.

Gallagher, J., and McLaughlin, D. (**1981**). "Experiments on the nonlinear characteristics of noise propagation from low and moderate Reynolds number supersonic jets," in *Proceedings of the 7th Aeroacoustics Conference, Aeroacoustics Conferences*, October 5–7, Palo Alto, CA.

Gee, K. L., Kenny, R. J., Neilsen, T. B., Jerome, T. W., Hobbs, C. M., and James, M. M. (**2012**). "Spectral and statistical analysis of noise from reusable solid rocket motors," Proc. Mtgs. Acoust. **18**(1), 040002.

Gee, K. L., Neilsen, T. B., Wall, A. T., Downing, J. M., James, M. M., and McKinley, R. L. (**2016**). "Propagation of crackle-containing jet noise from high-performance engines," Noise Control Eng. J. **64**(1), 1–12.

Gee, K. L., Russavage, P. B., Neilsen, T. B., Hales Swift, S., and Vaughn, A. B. (**2018**). "Subjective rating of the jet noise crackle percept," J. Acoust. Soc. Am. **144**(1), EL40–EL45.

Gurbatov, A. N., and Rudenko, O. V. (**2008**). "Statistical phenomena," in *Nonlinear Acoustics*, edited by M. F. Hamilton and D. T. Blackstock (Acoustical Society of America, Melville, NY).

Hamilton, M. F. (**2016**). "Effective Gol'dberg number for diverging waves," J. Acoust. Soc. Am. **140**(6), 4419–4427.

Leete, K. M., Vaughn, A. B., Bassett, M. S., Rasband, R. D., Novakovich, D. J., Gee, K. L., Campbell, S. C., Mobley, F. S., and Wall, A. T. (**2021**). "Jet noise measurements of an installed GE F404 engine," in *Proceedings of the AIAA Scitech 2021 Forum*, January 11–15 and 19–21.

McDaniel, O. H., Roth, S. D., and Welz, J. P. (**1980**). "Free-field propagation of high intensity noise," in *Proceedings of the Shock Noise Workshop*, December 5, Cleveland, OH.

McInerny, S. A., Gee, K., Downing, M., and James, M. (**2007**). "Acoustical nonlinearities in aircraft flyover data," in *Proceedings of the 13th AIAA/CEAS Aeroacoustics Conference (28th AIAA Aeroacoustics Conference)*, May 21–23, Rome, Italy.

McInerny, S. A., and Ölçmen, S. M. (**2005**). "High-intensity rocket noise: Nonlinear propagation, atmospheric absorption, and characterization," J. Acoust. Soc. Am. **117**(2), 578–591.

Morfey, C. L., and Howell, G. P. (**1981**). "Nonlinear propagation of aircraft noise in the atmosphere," AIAA J. **19**(8), 986–992.

Muhlestein, M., and Gee, K. (**2011**). "Experimental investigation of a characteristic shock formation distance in finite-amplitude noise propagation," Proc. Mtgs. Acoust. **12**(1), 045002.

Muhlestein, M. B. (**2013**). "Analyses of nonlinearity measures in high-amplitude sound propagation," Ph.D. thesis, Brigham Young University, Provo, UT.

Muhlestein, M. B., and Gee, K. L. (**2016**). "Evolution of the temporal slope density function for waves propagating according to the inviscid Burgers equation," J. Acoust. Soc. Am. **139**(2), 958–967.

Murray, N. E., and Lyons, G. W. (**2016**). "On the convection velocity of source events related to supersonic jet crackle," J. Fluid Mech. **793**, 477–503.

Pernet, D. F., and Payne, R. C. (**1971**). "Non-linear propagation of signals in airs," J. Sound Vib. **17**(3), 383–396.

Pestorius, F. M., and Blackstock, D. T. (**1974**). "Propagation of finite-amplitude noise," in *Finite-Amplitude Wave Effects in Fluids: Proceedings of the 1973 Symposium* (IPC Science and Technology, Guildford, UK), pp. 24–29.

Petitjean, B. P., Viswanathan, K., and McLaughlin, D. K. (**2006**). "Acoustic pressure waveforms measured in high speed jet noise experiencing nonlinear propagation," Int. J. Aeroacoust. **5**(2), 193–215.

Pineau, P., and Bogey, C. (**2021**). "Numerical investigation of wave steepening and shock coalescence near a cold Mach 3 jet," J. Acoust. Soc. Am. **149**(1), 357–370.

Reichman, B. O., Gee, K. L., Neilsen, T. B., and Miller, K. G. (**2016a**). "Quantitative analysis of a frequency-domain nonlinearity indicator," J. Acoust. Soc. Am. **139**(5), 2505–2513.

Reichman, B. O., Muhlestein, M. B., Gee, K. L., Neilsen, T. B., and Thomas, D. C. (**2016b**). "Evolution of the derivative skewness for nonlinearly propagating waves," J. Acoust. Soc. Am. **139**(3), 1390–1403.

Rudenko, O. V., and Chirkin, A. S. (**1975**). "Statistics of discontinuous noise waves in nonlinear media," Akad. Nauk SSSR Dokl. **225**, 520–523.

Sakagami, K., Aoki, S., Chou, I. M., Kamakura, T., and Ikegaya, K. (**1982**). "Statistical characteristics of finite amplitude acoustic noise propagating in a tube," J. Acoust. Soc. Jpn. E **3**(1), 43–45.

Shepherd, M. R., Gee, K. L., and Hanford, A. D. (**2011**). "Evolution of statistical properties for a nonlinearly propagating sinusoid," J. Acoust. Soc. Am. **130**(1), EL8–EL13.

Wall, A. T., Gee, K. L., James, M. M., Bradley, K. A., McInerny, S. A., and Neilsen, T. B. (**2012**). "Near-field noise measurements of a high-performance military jet aircraft," Noise Control Eng. J. **60**(4), 421–434.

Watanabe, Y., and Urabe, Y. (**1981**). "Changes of zero-crossing slopes of a finite-amplitude noise propagating in a tube," Jpn. J. Appl. Phys. **20**(S3), 35–39.

Webster, D. A., and Blackstock, D. T. (**1978**). "Experimental investigation of outdoor propagation of finite-amplitude noise," Technical Report NASA-CR-2992 (NASA Langley Research Center, Hampton, VA).

Webster, D. A., and Blackstock, D. T. (**1979**). "Amplitude density of a finite amplitude wave," J. Acoust. Soc. Am. **65**(4), 1053–1054.